

Supporting Information

Novel Geo-photocatalyst, an Iron-containing Layered Clay mineral for Photocatalytic H₂ Evolution from Water

Alisa Phuekphong,¹ Takayuki Hayakawa,² and Makoto Ogawa^{1,*}

¹School of Energy Science and Engineering, Vidyasirimedhi Institute of Science and Technology; 555 Moo 1 Payupnai, Wangchan, Rayong 21210, Thailand.

²Laboratory of Applied Clay Technology, Hojun Co., Ltd., An-naka, Gunma 379-0133, Japan.

Corresponding author: makoto.ogawa@vistec.ac.th

Table of contents

1. Experimental procedures	
1.1. Materials and chemicals	S2
1.2. Preparation of nontronite with varied interlayer cations	S2
1.3. Characterization	S2
1.4. Photocatalytic H ₂ evolution reaction	S3
2. Figures	S5
3. Tables	S12
4. References	S18

1. Experimental procedures

1.1. Material and chemicals

Materials and chemicals were used without further purification. Purified bentonite; Nontronite (Fe-clay), Bengel next LU and synthetic hectorite; Laponite were received by Hojun Co., Ltd. Tetraammineplatinum(II)nitrate (99.99%, Sigma-Aldrich), Silver nitrate (99.99%, Sigma-Aldrich), hydrochloric acid 37% and methanol for HPLC \geq 99.9% were purchased from Merck Co., Ltd. Deionized water was purified by using Milli-Q system (>18 M Ω cm, Millipore) before the use.

1.2. Preparation of Proton exchanged Fe-clay (H-Fe-clay)

H⁺ was exchanged with interlayer sodium cation of Fe-clay by ion exchange reaction in aqueous suspension. 0.5 g of Fe-clay was dispersed in 50 ml deionized water. Then, 0.1 M HCl was slowly added to the suspension until pH 3. The suspension was magnetically stirred at room temperature for 24 hours. The product was collected by centrifugation and washed with deionized water repeatedly until the negative silver nitrate test for chloride ion was obtained. Then, the product was dried in oven at 60°C and ground to obtain powder product.

1.3. Preparation of Pt nanoparticles immobilized H-Fe-clay

H-Fe-clay was used for the preparation of Pt-Fe-clay. Firstly, 0.1 g of H-Fe-clay was dispersed in 10 ml deionized water. Then, 1.98 mg of Pt(NH₃)₄(NO₃)₂ as Pt precursor was added to the suspension to prepare Pt-Fe-clay (1wt%). The suspension was magnetically stirred at room temperature for 24 hours. The product was collected by centrifugation and washed with deionized water. Then, the product was dried in oven at 60°C and ground to obtain powder product.

1.4. Characterization

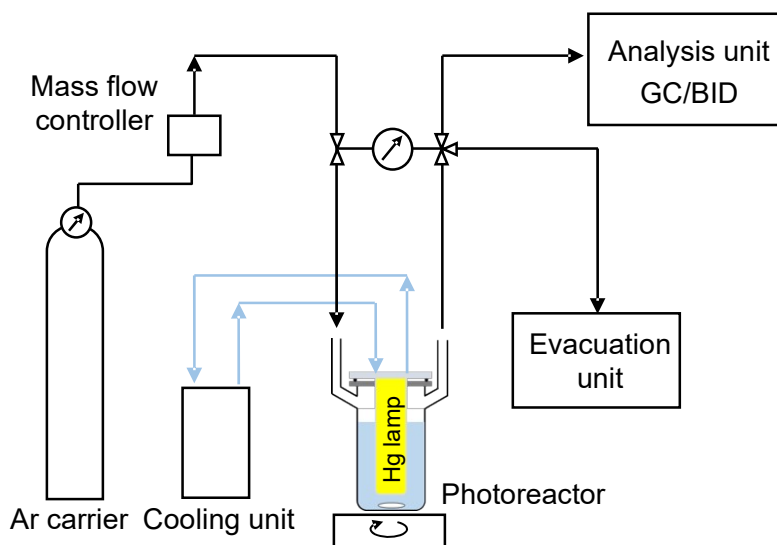
X-Ray diffraction (XRD) patterns were recorded using a Bruker New D8 Advance equipped with Ni filtered Cu K α radiation. Scanning electron micrographs were obtained on a JEOL JSM-7610F field-emission scanning electron microscopy (SEM) instrument. Prior to measurements, the samples were coated with platinum (thickness

of 4 nm). Elemental mapping images were obtained using an Oxford energy dispersive X-ray fluorescence spectrometer (X-Max 150 mm²) equipped with an SEM (JEOL, JSM-7610F). Transmission electron microscopy (TEM) and scanning transmission electron microscopy (STEM) images were obtained using a JEOL JEMARM200F high-resolution transmission electron microscope equipped with EDX analyzer microscope and was operated at 200 kV. The diffuse reflectance spectra were obtained by using UV spectrometer (Perkin Elmer Lambda 1050 UV/Vis/NIR Spectrophotometer) with an integrated sphere. The elemental composition of the sample was analyzed by a wavelength-dispersive X-ray fluorescence spectrometer (WDXRF, Bruker S8 Tiger). The chemical surface analysis was evaluated by X-ray photoelectron spectroscopy (XPS, JPS-9010MC, JEOL) with Mg–K α radiation source ($h\nu = 1253.6$ eV). Thermogravimetric analysis was performed using Linseis STA PT1600 at the heating rate of 10 °C/min under an air atmosphere. The amount of Fe in supernatant after photocatalytic reaction was determined by inductively coupled plasma-optical emission spectroscopy analysis (700 Series ICP-OES, Agilent Technologies, Santa Clara, CA, USA) and the calibration curve (R factor >0.999) was made for Fe measurement using standard Fe(III) nitrate; Fe(NO₃)₃ solution. N₂ adsorption/desorption isotherms were obtained at –196 °C on a BELSORP mini instrument (MicrotracBEL Corp). Prior to the measurement, samples were dehydrated at 100 °C under vacuum for 3 h. The surface area was calculated using the Brunauer–Emmett–Teller (BET) method.

1.5. Photocatalytic hydrogen evolution experiment

Photocatalytic reaction was carried out in a closed gas-circulation system with 250 ml Pyrex glass reactor and 400 W high-pressure Hg lamp as the light source (HL400BH-8, SenLights Co., Ltd. $\lambda_{\text{max}} = 365$ nm). Photocatalyst (50 mg) was dispersed in 100 ml of water (for pure water system) and aqueous MeOH (10%v/v) as sacrificial agent. (The amount of photocatalyst was optimized from aqueous MeOH (10%v/v) at 3 hours after light irradiation by a preliminary experiment in which varied amounts of photocatalyst was used.) The suspension was evacuated several times prior to the irradiation in order to remove remaining O₂ and N₂ gases in photoreactor and suspension. The suspension was kept at 25°C by using circulated cooling water. The evolved H₂ was analyzed using

gas chromatography equipped with BID detector (GC-2010Plus A(BID), Shimadzu) equipped with 5A° molecular sieve column. The photocatalytic experimental set-up was illustrated as follows,



Photocatalytic reaction set-up

For the evolution of the stability of the photocatalyst, photocatalytic reaction was carried out repeatedly. The suspension was irradiated 3 hours for each cycle with the sampling time interval of 1 hour. After that, the evolved gases in photoreactor were evacuated before starting the new cycle. After the photocatalytic reaction, the used photocatalysts were collected by centrifugation and then dried in oven at 60°C.

2. Figures

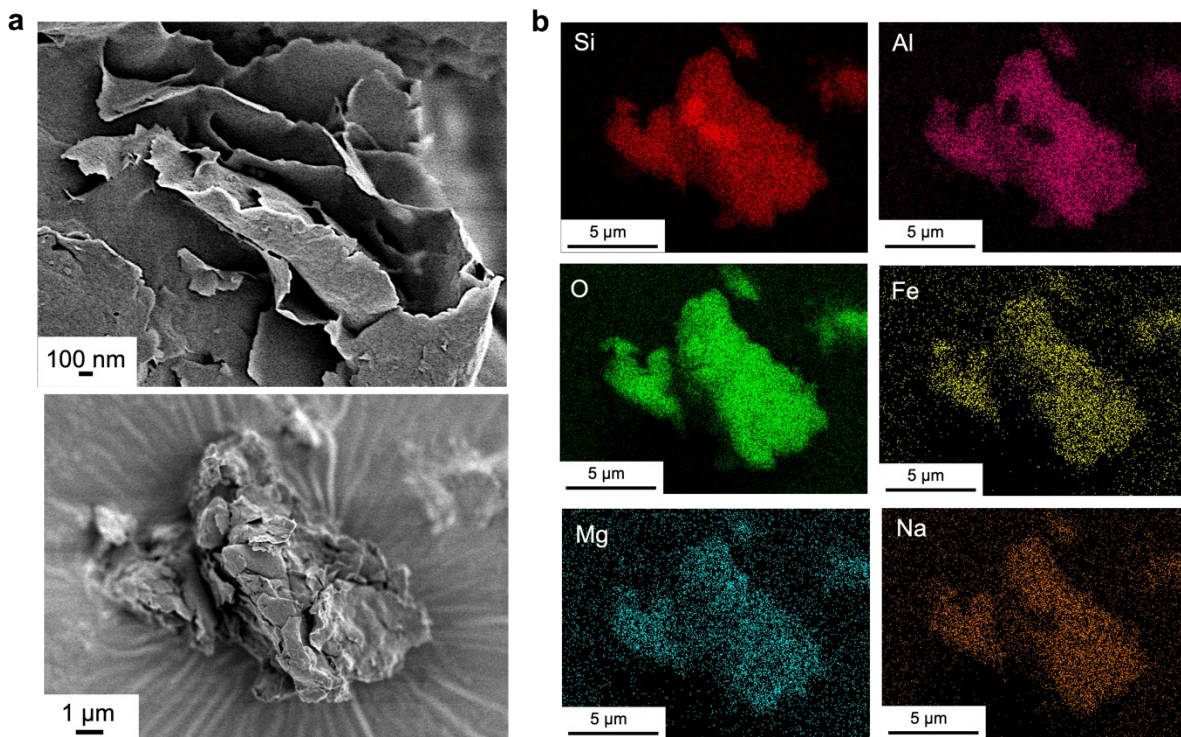


Fig. S1 (a) Scanning electron microscopy (SEM) images and (b) elemental analysis of Fe-clay.

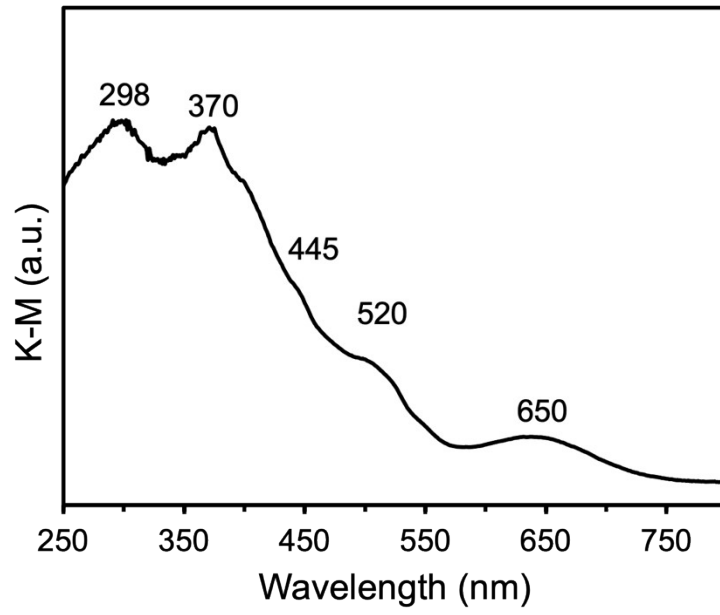


Fig. S2 UV-vis diffuse reflectance spectrum of Fe-clay.

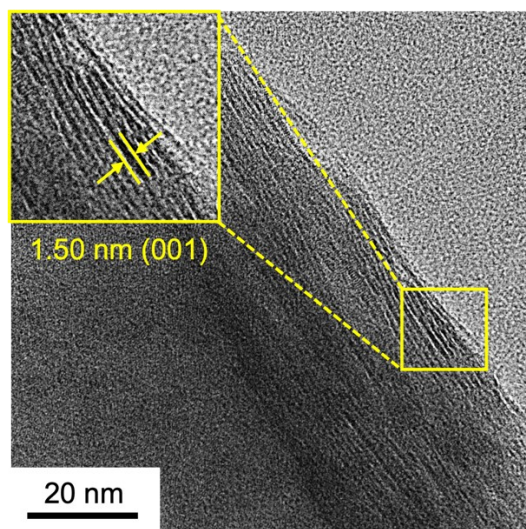


Fig. S3 TEM image of H-Fe-clay (inset: showing lattice fringes).

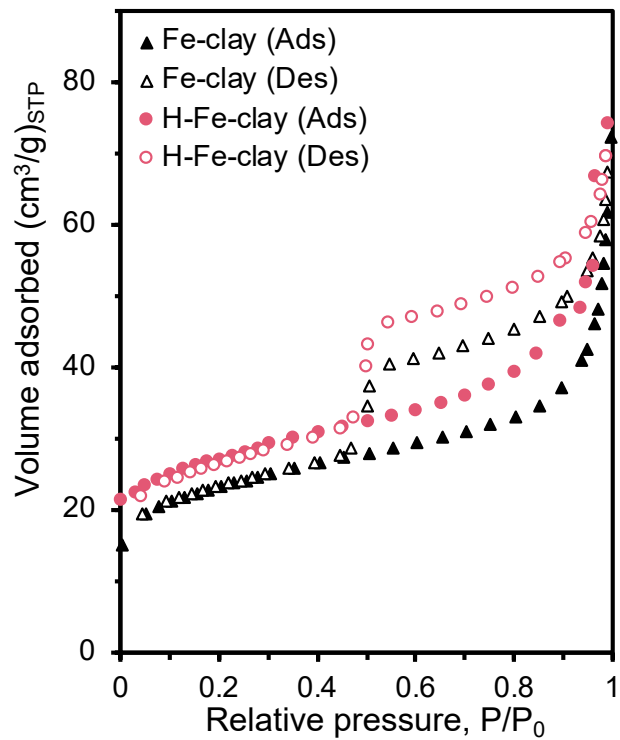


Fig. S4 N₂ adsorption-desorption isotherms of Fe-clay (black triangle) and H-Fe-clay (red circle).

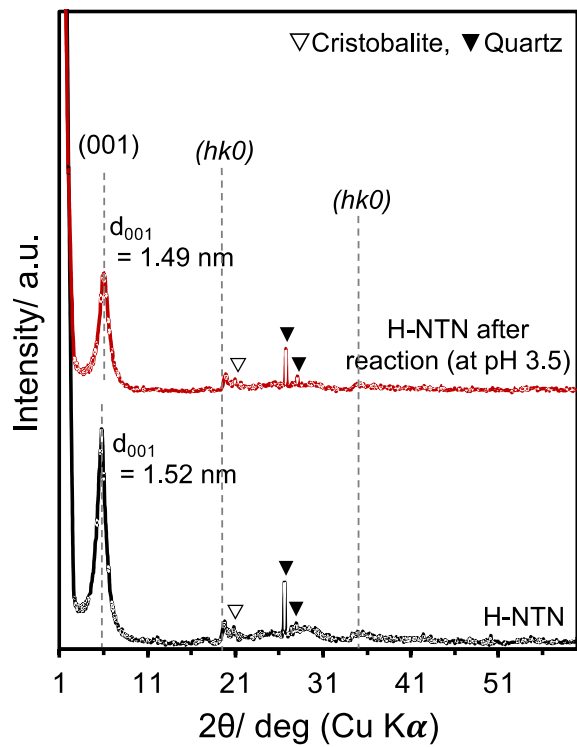


Fig. S5 X-Ray diffraction patterns of H-Fe-clay before and after the photocatalytic reaction at pH 3.5.

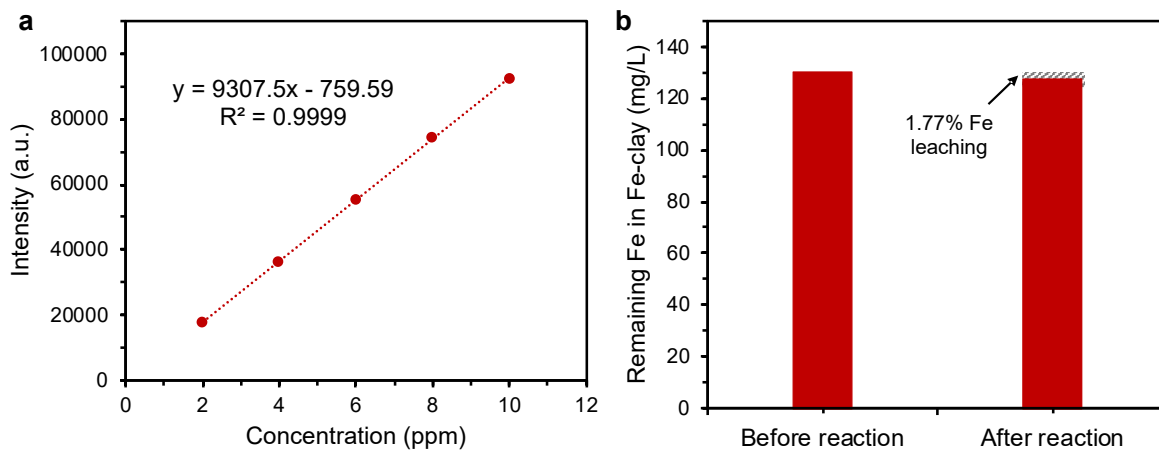


Fig. S6 (a) Calibration curve of Fe for ICP analysis, and (b) remaining Fe in Fe-clay before and after the reaction (derived from ICP analysis of supernatant after photocatalytic reaction for 6 h, 1 cycle).

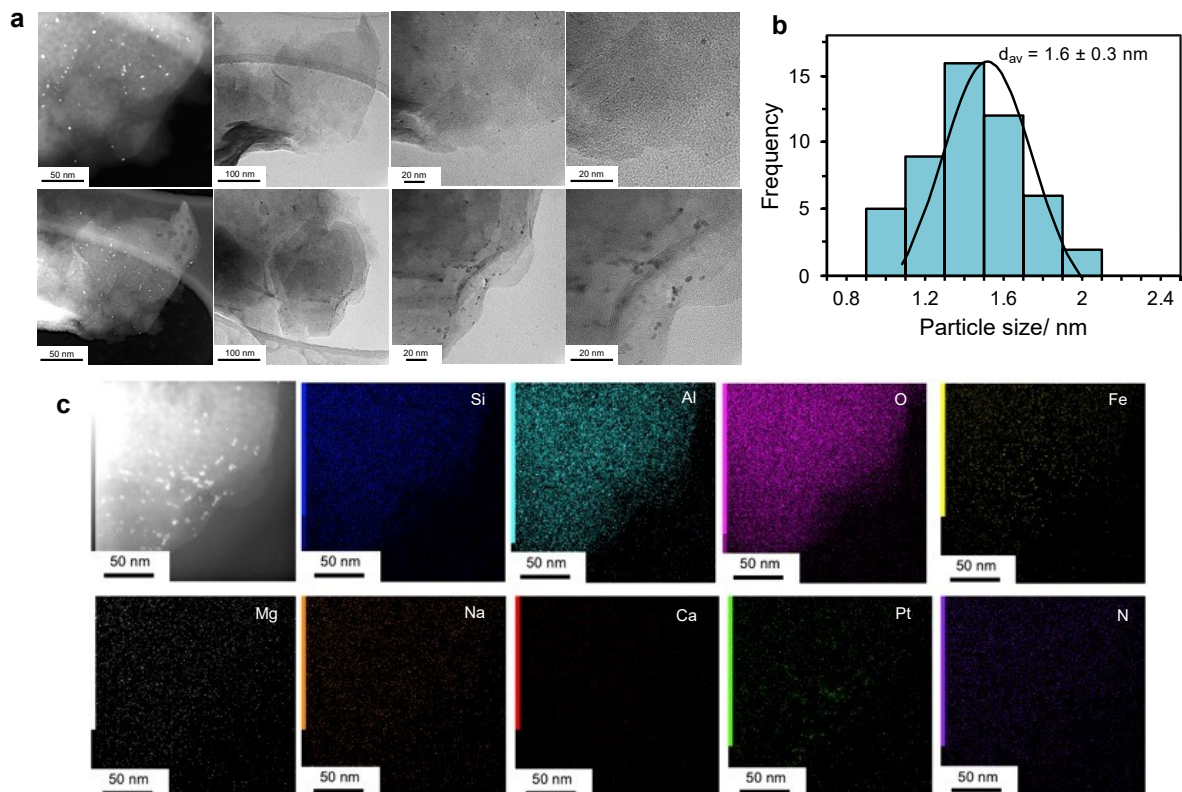


Fig. S7 (a) TEM images, (b) particle size distribution of Pt nanoparticles, and (c) STEM and elemental mapping of 1wt% Pt-Fe-clay after photocatalytic H₂ evolution tests for 9 cycles.

3. Table

Table S1. Elemental composition of Fe-clay analyzed by X-ray fluorescence spectroscopy.

Composition	Content/ wt%
SiO ₂	55.9
Al ₂ O ₃	16.4
Fe ₂ O ₃	16.4
Na ₂ O	3.23
MgO	2.81
CaO	2.20
TiO ₂	1.84
K ₂ O	0.85
Fe/Si ratio	0.29

Table S2. Assignment of absorption position from UV-vis diffuse reflectance spectra of Fe-clay.

Absorption position/ nm	Assignment of absorption position			
	S. W. Karickhoff [1]	D. Bonnin [2]	R. B. Merola [3]	D. M. Sherman [4]
298	-	O ²⁻ → Fe(III) charge transfer	-	O ²⁻ → Fe(III) charge transfer
370	Oct Fe(III), ⁶ A _{1g} → ⁴ E _g (D)	Oct Fe(III), ⁶ A _{1g} → ⁴ E _g (D)	-	Oct Fe(III), ⁶ A _{1g} → ⁴ E _g (D)
445	Oct Fe(III), ⁴ A _{1g} → ⁴ A ₁ ⁴ E(G)	Oct Fe(III), ⁶ A _{1g} → ⁴ E _g (G)	-	Oct Fe(III), ⁶ A _{1g} → ⁴ T ₁ (G)
520	Oct Fe(III), ⁶ A _{1g} → ⁴ T ₂ (G)	-	Oct Fe(III), ⁶ A _{1g} → ⁴ T ₂ (D)	-
650	-	Oct Fe(III), ⁶ A _{1g} → ⁴ T ₂ (G)	Tet Fe(III), ⁶ A _{1g} → ⁴ T ₁ (G)	Oct Fe(III), ⁶ A _{1g} → ⁴ T ₂ (G)
667-715	-	-	-	Fe(II) → Fe(III) charge transfer

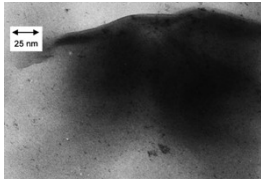
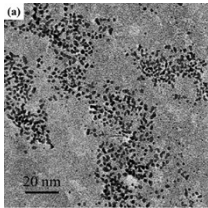
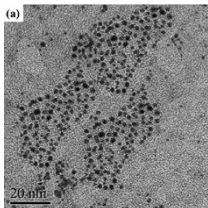
Table S3. Iron content and interlayer characteristic of Fe-clay, Bengel next LU and Synthetic hectorite (Laponite).

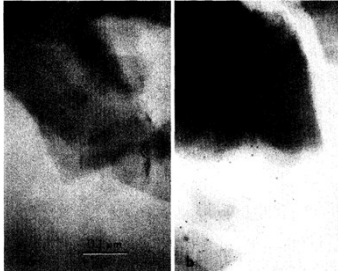
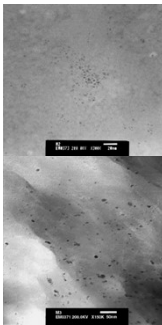
Sample	Fe content/ wt%	Interlayer cation	$d_{(001)}$ spacing/ nm	CEC/ meq/100g	Source
Fe-clay	16.4	Na ⁺	1.28	100	Hojun Co., Ltd.
Bengel next LU	1.51	Na ⁺	1.25	82	Hojun Co., Ltd.
Laponite	-	Na ⁺	1.25	55	Rockwood Industries

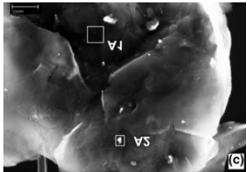
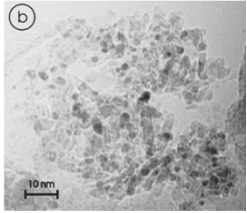
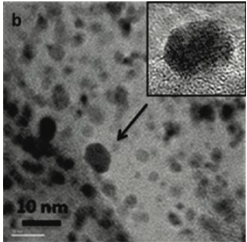
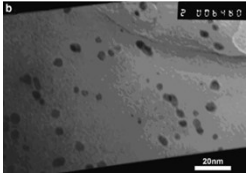
Table S4. Elemental composition of H-Fe-clay and 1wt% Pt-Fe-clay before/ after performing photocatalytic reaction. (H-Fe-clay (pH 3.5) at 6 hours, 1 run and 1wt% Pt-Fe-clay at 27 hours, 9 runs)

Composition (oxide)	Before the reaction		After the reaction	
	H-Fe-clay	1wt% Pt-Fe-clay	H-Fe-clay (pH 3.5)	1wt% Pt-Fe-clay (recycle test)
SiO ₂	55.6	52.6	58.1	57.4
Al ₂ O ₃	17.3	20.4	18	17.9
Fe ₂ O ₃	16.2	15.6	15.8	15.7
Na ₂ O	2.5	2.0	1.18	1.2
MgO	2.9	3.0	2.4	2.9
CaO	1.8	1.6	1.8	1.4
TiO ₂	2.1	1.5	1.4	1.5
K ₂ O	0.8	1.1	0.8	0.5
Pt	-	1.5	-	1.1
Fe/Si ratio	0.29	0.29	0.27	0.27

Table S5. Previous reports on preparation of platinum nanoparticles supported on clay minerals.

Ref.	Clay/ Clay mineral	Method	d_{001} spacing/ nm	%Loading	Average size of Pt/ nm	TEM images
[5]	Montmorillonite (MMT)	1. Ion exchange with dihydrocinchonidine hydrochloride (DHCd·HCl)	MMT = 1.29 DHCd-MMT = 1.37 Pt-DHCd-MMT not changed	2 %wt	0.8 Distribution (0.3-1.8 nm)	
	Hectorite (Hec)	2. Impregnation of $H_2[PtCl_6]^{2-}$ 3. Reduction with $NaBH_4$				Hec = 1.55 DHCd-Hec = 1.68 Pt-DHCd-Hec not changed
[6]	Hectorite (Hec)	1. Dispersion of clay in H_2O 2. Addition of $K_2[Pt(Cl_4)]^{2-}$ 3. <i>In situ</i> reduction at RT induced by silanol group of clay	Hec = 1.38 Pt-Hec = 1.38, not changed	5.0 %wt	Distribution (3-6 nm)	
				5.0 %wt	Distribution (2-6 nm)	

[7]	Montmorillonite	<ol style="list-style-type: none"> 1. Ion exchange with $(\text{NO}_3)_2[\text{Pt}(\text{NH}_3)_4]^{2+}$ 2. Reduction with H_2, 140°C 	$[\text{Pt}(\text{NH}_3)_4]^{2+}$ -MMT = 1.26 Pt-MMT = 1.07	0.6 %wt 1.0 %wt 3.0 %wt	2.3 Distribution (1-4 nm) 4.3 Distribution (1-6 nm) 9.8 Distribution (1-10 nm)	
[8]	Montmorillonite	<ol style="list-style-type: none"> 1. Preparation solution of CTAB + $\text{H}_2[\text{Pt}(\text{Cl}_6)]^{2-}$ 2. Reduction with NaBH_4 (obtained Pt hydrosol) 3. Addition Pt hydrosol to clay suspension 	MMT = 1.47 CTA-MMT = 5.92 Pt-CTA-MMT = 5.92, not changed	1.0 %wt 2.0 %wt	2.7 Distribution (1.7~3.8 nm) 9.0 Distribution (5~11 nm)	
[9]	K-10 montmorillonite	<ol style="list-style-type: none"> 1. Dispersion of clay in aqueous solution 2. Impregnation of $\text{H}_2[\text{Pt}(\text{Cl}_6)]^{2-}$ 3. Reflux in EtOH (reduction) 	MMT ~ 1 nm Pt-MMT not changed	5.0 %wt	3.8 Distribution (2-10 nm)	-
[10]	Bentonite	<ol style="list-style-type: none"> 1. Ion exchange with $(\text{NO}_3)_2[\text{Pt}(\text{NH}_3)_4]^{2+}$ 2. Reduction with H_2 at 25°C, 300°C, 400°C 	BT = 1.25 $[\text{Pt}(\text{NH}_3)_4]^{2+}$ -BT = 1.41 Pt-BT/ 25°C = 1.51 Pt-BT/ 300°C = 1.47 Pt-BT/ 400°C = 1.00	1.0 %wt	Not determined	-

[11]	Montmorillonite	<ol style="list-style-type: none"> 1. Preparation of $C_{18}H_{37}N^+$ + $H_2[PtCl_6]^{2-}$ solution 2. Reduction with $NaBH_4$ 3. Addition of clay to Pt suspension 	C_{18} -MMT = 2.61 Pt- C_{18} -MMT = 2.69	1.0 %wt 5.0 %wt	9.2 21.6 *Observed from FESEM	 (M) (FESEM)
[12]	Bentonite	<ol style="list-style-type: none"> 1. Ion exchange with $(NO_3)_2[Pt(NH_3)_4]^{2+}$ 2. Ion exchange with dihydrocinchonidine hydrochloride 3. Reduction with $NaBH_4$ 	BT = 1.26 Pt-BT = 1.73	1.0 %wt	1.5 Distribution (0.6-2.6 nm)	
[13]	Montmorillonite (Cloisite Na ⁺) Organically modified montmorillonite (Cloisite 20A)	<ol style="list-style-type: none"> 1. Chemical vapor deposition of $Pt^{2+}[(O_2C_5H_7)_2]$ on Cloisite and Cloisite 20A at 350°C 2. Calcination at 350°C, 8h 3. Reduction with H_2/Ar gas at 350°C, 4h 	Cloisite20A = 2.42 Pt-Cloisite20A = absence	4.17 %wt	3.74±0.69 nm	
[14]	Montmorillonite	<ol style="list-style-type: none"> 1. Preparation of clay + $H_2[PtCl_6]^{2-}$ suspension in MeOH 2. Transferred to autoclave, flushed with N_2, heat at 300°C (under supercritical state of MeOH to reduce Pt precursor) 	MMT = 1.25 Pt-MMT = 1.48	Not determined	Distribution (2-12 nm)	

4. References

- [1] S. W. Karickhoff, G. W. Bailey, *Clays Clay Miner.* 1973, **21**, 59–70.
- [2] D. Bonnin, G. Calas, H. Suquet, H. Pezerat, *Phys. Chem. Miner.* 1985, **12**, 55–64.
- [3] R. B. Merola, M. M. McGuire, *Clays Clay Miner.* 2009, **57**, 771–778.
- [4] D. M. Sherman, N. Vergo, *Am. Miner.* 1988, **73**, 1346–1354.
- [5] Á. Mastalir, G. Szöllösi, Z. Király, Z. Rázga, *Appl. Clay Sci.* 2002, **22**, 9–16.
- [6] D. Varade, K. Haraguchi, *Langmuir* 2013, **29**, 1977–1984.
- [7] J. B. Harrison, V. E. Berkheiser, G. W. Erdos, *J. Catal.* 1988, **112**, 126–134.
- [8] D. Manikandan, D. Divakar, A. V. Rupa, S. Revathi, M. E. L. Preethi, T. Sivakumar, *Appl. Clay Sci.* 2007, **37**, 193–200.
- [9] G. Szöllösi, B. Török, L. Baranyi, M. Bartók, *J. Catal.* 1998, **179**, 619–623.
- [10] G. Szöllösi, I. Kun, Á. Mastalir, M. Bartók, I. Dékány, *Solid State Ionics* 2001, **141**, 273–278.
- [11] H. A. Patel, S. Bocchini, A. Frache, G. Camino, *J. Mater. Chem.* 2010, **20**, 9550–9558.
- [12] G. Szöllösi, Á. Mastalir, Z. Király, I. Dékány, *J. Mater. Chem.* 2005, **15**, 2464–2469.
- [13] W. Zhang, M. K. S. Li, R. Wang, P. Yue, P. Gao, *Langmuir* 2009, **25**, 8226–8234.
- [14] J. Pen, J. Liu, S. Guo, Z. Yang, *Catal. Lett.* 2009, **131**, 179–1